Analysis of protein–protein interaction by simulation of small-zone size exclusion chromatography

Stochastic formulation of kinetic rate contributions to observed high-performance liquid chromatography elution characteristics

Fred J. Stevens
Biological, Environmental, and Medical Research Division, Argonne National Laboratory, Argonne, Illinois 60439-4833

ABSTRACT High-performance liquid chromatography (HPLC) procedures provide size-exclusion chromatography with sufficient speed that the elution characteristics of mixtures of interacting macromolecules are potentially determined by the kinetics of association and dissociation. However, few studies have yet addressed the consequences of interaction kinetics on HPLC analyses or evaluated the potential application of HPLC methods for the qualitative and quantitative interpretation of macromolecular interaction kinetics. An earlier simulation of small-zone chromatography of interacting molecules (Stevens, F. J. 1986. *Biochemistry.* 25:981–993) has been modified to incorporate the effects of association/dissociation kinetics on elution behavior. The previous assumption of instantaneous equilibration has been replaced by explicit calculation of partial relaxation of complexed and free constituent mixtures during each iteration of the simulation. In addition, a stochastically based formulation has been introduced to determine a velocity probability distribution that emulates the partial intermixing of free and complexed pools during the iteration cycle. The simulation generates bimodal elution profiles representing stable complexed and free components of mixtures for which interaction is characterized by slow kinetics relative to chromatography run times. For mixtures with rapid kinetics, a single asymmetric peak results. When tested with a large-zone sample such that a plateau of stable concentration is generated, the simulation reproduces previous characterizations based on evaluations of solute continuity equations. Therefore, HPLC may, in many cases, be an appropriate basis for techniques by which to evaluate kinetic and affinity characteristics of interacting biomolecules.

INTRODUCTION

Analytical models to describe transport properties of interacting macromolecules during processes such as sedimentation, chromatography, and electrophoresis have been developed by several authors. Traditionally, models were based on the concept of "instantaneous equilibration" (1–8). Cann and co-workers (4, 9, 10) and Zimmerman (11) introduced rate constants into their zonal transport calculations and determined conditions under which observed sedimentation or chromatographic elution profiles would be kinetically controlled. Endo and co-workers (12, 13) have described a "zone interference" technique that yields interaction rate constants under certain circumstances when one of the interacting components is present in sufficient excess to provide first-order kinetics.

Rapid equilibrium was also explicitly assumed in an iterative simulation of small-zone, size-exclusion chromatography described previously (14). This assumption was probably satisfactory for the experimental system that was the focus of that study. The affinity constant for the interaction between the antigen-binding fragment (Fab) of a rheumatoid factor IgA and the antigenic Fc portion of an IgG was estimated to be $\sim 10^5$ M^{-1}. Assuming a typical association rate constant of $\sim 10^5$ M^{-1} s^{-1}, the dissociation rate constant was near unity, assuring that the time period represented by each iteration cycle of the simulation was long relative to the dissociation half-life of the reaction.

For several reasons, instantaneous equilibration is not an appropriate assumption upon which to base an interaction simulation that is intended to have systematic application for chromatographic analyses of interacting macromolecules. (*a*) The affinities of interaction between antibodies and antigens, for instance, can range from 10^4 to 10^{10} M^{-1}. Because a typical forward rate constant for an antibody/antigen interaction can be taken as 10^5 M^{-1} s^{-1}, reverse rate constants between 10 and 10^{-5} s^{-1} can be anticipated. As a consequence, in an experimental study of a series of antibodies directed against a specific antigen, one may expect to find cases in which instantaneous equilibration (14), partial equilibration, or null equilibration (15) may each be demonstrated. (*b*) Contemporary high-performance liquid chromatography (HPLC)–based size-exclusion columns provide for run times of a few minutes, in which even equilibration rates conventionally considered rapid may be slow relative to the time required for completion of the run. (*c*) The "reality" of numerical simulation, in general, improves with increased number of iterations per simulation run. In the chromatography simulation, each iteration cycle represents a

small time element. Therefore, if an assumption of instantaneous equilibration is imposed upon an interacting macromolecular system that exhibits partial equilibration, the resulting error is increased as the number of iterations representing the complete column run is increased. (*d*) The leading and trailing edges of the solute peak in large-zone chromatography and the entire solute band in small-zone chromatography represent concentration gradients. Because the half-life for equilibration of the interacting molecules is determined by the forward rate constant in combination with the reactant concentrations, it is clear that, in principle, the microzonal relaxation time is different at each point of the solute gradient(s). As a consequence, the magnitude of the error resulting from the instantaneous equilibration assumption is not uniform and can lead to unanticipated distortion of predicted elution profiles.

This report describes an iterative simulation in which the elution behavior of small-zone interacting solutes is determined by the rate constants of association and dissociation. The simulation is based on that described previously (14); modifications include calculation of partially equilibrated constituent populations after each translation step in the simulation. A new algorithm is incorporated to approximate an effective velocity distribution function that results from partial intermixing of free and complexed solute pools because of multiple interactions during the iteration time element. Simulated chromatograms exhibit elution characteristics sensitively linked to association and dissociation rates. The contribution of kinetic rate parameters to elution behavior is modulated by chromatographic run time and solute concentrations.

METHODS

Stochastic kinetics

Consider the reversible reaction

$$A + B \underset{k_r}{\overset{k_f}{\rightleftharpoons}} C. \tag{1}$$

At each instant,

$$\frac{dc}{dt} = k_f ab - k_r c, \tag{2}$$

in which a, b, and c are the molar concentrations of free and complexed components.

During the time element δt, individual molecules of A and B exist in free form or in the complexed form C. The fraction of C that remains complexed during δt is controlled by the dissociation rate constant k_r; likewise, the fractions of A and B that remain free are determined by the forward rate constant k_f in conjunction with the concentrations a and b.

At times $t = t_o$ and $t = t_o + \delta t$, the composition of the A, B mixture may be regarded as partitioned between pools of free molecules and the pool of complexed molecules. To model the elution characteristics of the total population of each elemental cell of the simulated chromatography column, it is necessary to determine the extent of intermixing between the two pools during the interval δt although this consideration was evidently not incorporated in a recent adaptation (16) of the earlier simulation (14) or in other approaches (17, 18) to simulation of kinetic aspects of small-zone transport. Consider, for instance, two reaction mixtures at the same constituent concentrations and characterized by the same affinity constants. The affinity constant is the ratio of forward and reverse rate constants; therefore, let sample 1 be characterized by slow reaction kinetics so that

$$(k_{1f}ab)\delta t = (k_{1r}c)\delta t \approx 0. \tag{3}$$

In contrast, imagine sample 2 to be characterized by rapid kinetics such that

$$(k_{2f}ab)\delta t = (k_{2r}c)\delta t \gg c. \tag{4}$$

Eq. 4 indicates that the number of reactions occurring during the time interval δt greatly exceeds the number of molecules present, thereby resulting in each molecule participating in multiple dissociation and association reactions. On this basis, sample 2 may be considered to express 'instantaneous equilibration' in accord with the standard assumption underlying many transport analyses. Despite equal affinity constants, the elution behaviors of samples 1 and 2 are distinct. Sample 1 is translated as two separate and independent populations of free and complexed constituents; sample 2 is translated as a single homogeneous population of intermediate velocity.

The intermixing between free and complexed pools is calculated from the integrated flux between the two pools, i.e., the total number of association/dissociation reactions that occur during the time-interval δt. At time t, the concentration of complex is obtained from the standard kinetic relaxation expression,

$$c(t) = \bar{c} + (c - \bar{c})_o \exp[-t/\tau], \tag{5}$$

where $\bar{c}$ is the equilibrium concentration of complex, $(c - \bar{c})_o$ is the displacement from equilibrium at time $t = 0$, and τ is the relaxation time given by

$$\tau^{-1} = k_f(\bar{a} + \bar{b}) + k_r. \tag{6}$$

The probability that a free component undergoes an association can be determined from the average number of association reactions experienced by each constituent. This average value is obtained from the number of association reactions divided by the total concentration of the constituent available for reaction, i.e., the concentration of free component. Assuming that the reaction flux is approximately constant during the short time interval represented by δt, the number of association reactions may be estimated:

$$n_a = \frac{k_f ab\delta t}{a} = k_f b\delta t, \tag{7}$$

and

$$n_b = k_f a\delta t. \tag{8}$$

Association reactions are considered to be random, independent events distributed uniformly through the population of molecules. Therefore, the probability that a given free A or B molecule does not associate, i.e., receives zero association events, may be calculated from the Poisson probability distribution,

$$pA_j(0, n) = \frac{n_j^0 \exp[-n_j]}{0!} = \exp[-n_j], \tag{9}$$

whre n_j refers to the average number of association events per A or B molecule. The concentration-dependent probabilities of association are therefore:

$$pA_a = 1 - \exp\ [-k_f b \delta t] \tag{10}$$

$$pA_b = 1 - \exp\ [-k_f a \delta t]. \tag{11}$$

The time-dependent probability distribution function for dissociation is taken to be that given by first-order dissociation kinetics,

$$pD_c = 1 - \exp\ [-k_r \delta t]. \tag{12}$$

Note that this expression is also the Poisson probability for at least one dissociation event, given that $k_r \delta t$ represents the average number of dissociation events per complex during interval δt.

Constituent velocity distribution

Each iteration cycle comprises a duration equal to the run time divided by the number of iteration cycles in the simulated run. In the previous simulation formulation that assumed complete reequilibration, each translation step was followed by a calculation of a new equilibrium composition of free and complexed components in each elemental cell. Because instantaneous equilibration implies complete admixture of free and complex pools, the characteristic velocity of the content of an elemental cell was determined from weighted average velocities of free and aggregate species.

In the current case, explicit incorporation of the kinetic rate constants results in two direct consequences: (*a*) incomplete equilibration and (*b*) partial rather than complete interchange between pools of free and aggregated molecules. The first consideration is dealt with directly by use of Eqs. 5 and 6, in which $\bar{c}$, the equilibrium complex concentration, is obtained from the unitless total constituent concentrations a'_o and b'_o ($a'_o = K_a a_o$, $b'_o = K_a b_o$) by

$$\bar{c} = [(1 + a'_o + b'_o) - \sqrt{(1 + a'_o + b'_o)^2 - 4a'_o b'_o}]/2K_a \tag{13}$$

and

$$\bar{a} = a_o - \bar{c} \tag{14}$$

$$\bar{b} = b_o - \bar{c}. \tag{15}$$

Eq. 5 provides the concentration of complex at the end of time interval δt. However, the net change in complex concentration does not directly reveal the translation characteristics of the sample during the time interval. If the rate of relaxation is sufficiently rapid to justify an assumption of instantaneous equilibration, then the translation rate of the mixture is represented by a weighted average of free molecule and complex constituent velocities (14). Incomplete relaxation results in partial intermixing of the free and complexed forms. Molecules experience varying durations in aggregate form during the cycle. Therefore, a velocity distribution function more closely represents the translational characteristics of each pool during the iteration cycle than does explicit constituent velocities or averaged intermediate velocities.

An algorithm to develop the kinetically determined velocity distribution was based on subdividing the iteration cycle into K subintervals and postulating that a transition between free and complexed form occurs only at the initiation of the subinterval. During a subinterval, a molecule is either discretely free or complexed. The monomeric [1] or complexed [0] state of a molecule is conveniently represented by a string of zeros and ones. All possible 'history lines' (19) are systematically generated by a sequence of binary numbers. The effective velocity corresponding to each history line is determined by summation of the elements of the string. This process is illustrated in Table 1 for an iteration cycle parsed into three subintervals, generating 2^3 history lines for molecules in monomer or complex state at time $t = 0$ (subinterval $k = 0$). Subpopulations a [(0)000] and a' [(1)000] are each translated with velocity $v = v(0)$ (velocity of complex). However, the probabilities associated with the two subpopulations are not the same. The initial event for the two history lines is different; a *not-dissociate* probability is required for subpopulation a but an *associate* probability is needed for the initial transition from monomer to dimer for subpopulation a'. Subpopulations for which the summed velocities $\sigma_v = 1$ (b, c, e, b', c', e') are translated with proportional velocity $[1 \cdot v(1) + 2 \cdot v(0)]/3$, etc.

The relative number of binary strings that generate each σ_v can be immediately calculated from a binomial distribution. However, the binomial distribution cannot be used directly to calculate the relative occupancy of each σ_v because not all subpopulations occur with equal probability. The velocity distribution $[c(\sigma_v)]$ defines the concentration of complex or free molecule that translates with proportional velocity corresponding to σ_v. In this example, the velocity distribution for complexes is given by the expression

$$c(0) = c \cdot [P(a)] \tag{16}$$

$$c(1) = c \cdot [P(b) + P(c) + P(e)] \tag{17}$$

$$c(2) = c \cdot [P(d) + P(f) + P(g)] \tag{18}$$

$$c(3) = c \cdot [P(h)], \tag{19}$$

where $P(x)$ refers to the probability of history line x, noting that

$$\sum_{x=a}^{h} P(x) = 1. \tag{20}$$

The corresponding velocity distribution for the free molecule population is obtained by substituting the free solute concentration, a or b, for that of the complex.

The probability $P(x)$ is evaluated by converting each history line into a corresponding string of events that are required to generate it. For instance, $P(g)$ in Table 1 is represented by the history line (0)011, which converts to the event line $\bar{d}d\bar{a}$ representing the event string: *not-dissociate/dissociate/not-associate*. $P(g)$, therefore is given by the probability product:

$$P(g) = (1 - pD)pD(1 - pA). \tag{21}$$

Bivalent interactions may be modeled in a similar manner. In this

TABLE 1 History line representation

	k*						k				
p‡	0	1	2	3	σ_v§	p	0	1	2	3	σ_v
a	(0)	0	0	0	0	a'	(1)	0	0	0	0
b	(0)	1	0	0	1	b'	(1)	1	0	0	1
c	(0)	0	1	0	1	c'	(1)	0	1	0	1
d	(0)	1	1	0	2	d'	(1)	1	1	0	2
e	(0)	0	0	1	1	e'	(1)	0	0	1	1
f	(0)	1	0	1	2	f'	(1)	1	0	1	2
g	(0)	0	1	1	2	g'	(1)	0	1	1	2
h	(0)	1	1	1	3	h'	(1)	1	1	1	3

*k, subinterval index.
‡p, subpopulations originally in complexed form (0) indicated by unprimed labels, in free form (1) indicated by primed labels.
§σ_v, summed subintervals as free molecule.

case, history lines are generated in which each subinterval represents one of three states: unbound, singly bound, or double bound. As a result, three subintervals generate 27 history lines in contrast to the eight history lines obtained for monovalent interaction. In addition, each transition between subintervals represents a probability product or sum of probability products, as opposed to a single probability necessary for a monovalent interaction transition. For instance, if 0, 1, and 2 indicate unbound, singly bound, and doubly bound states, respectively, the transition represented by 1 → 2 requires the product (*associate*) · (*not-dissociate*), whereas the transition 1 → 1 is represented by sum of products (*associate*) · (*dissociate*) + (*not-associate*) · (*not-dissociate*). Simulation of small-zone chromatography of bivalent interactions under kinetic control represents significant, but manageable, additional computational complexities and will be the subject of future study.

Chromatography simulation

The simulation algorithm is similar to that described previously (14). In brief, the chromatography column is considered to be a linear array of elemental cells. The sample mixture is assumed to be at equilibrium at the time of introduction to the column. Transport is effected by Gaussian translation of cell content to succeeding cells. The constituent velocity of a solute represents the mean translation, and the standard deviation of the distribution introduces a dispersion factor into the transport process. The translation step is followed by a diffusion step after which the free and complexed composition of each cell is recalculated. This cycle is repeated until the sample is completely eluted from the column. In the original algorithm, equilibration was assumed to be rapid and complete. Therefore, no absolute time duration was attributed to an iteration cycle in the original algorithm.

The translation algorithm of the current simulation was altered to incorporate the kinetic formulation described above. For free constituents and complex at the beginning of the iteration interval, separate $N \times K$ velocity distribution tables are generated that consist of velocity distribution functions obtained at N values of pA. Values of pA range from 0.0 to 1.0 and are obtained for history lines containing $K - 1$ subintervals representing K discrete velocities ranging from that of free constituent to that of the complex. These tables are constructed during the initialization stage of the program and are dependent upon the specific value of k_r characteristic of the reaction under study.

Eq. 18 represents the subpopulation of complexes that translate with effective velocity 1.33 during an iteration interval. The relevant history lines associated with this subpopulation are (0)110, (0)101, and (0)011 and correspond to the event lines $d\bar{a}a$, dad, and $\bar{d}d\bar{a}$. If, for instance, $pA = 0.1$ and $pD = 0.4$, then the probability associated with a complex of effective velocity 1.33 is simply $(0.4)(1 - 0.1)(0.1) + (0.4)(0.1)(0.4) + (1 - 0.4)(0.4)(1 - 0.1) = 0.268$. Since an effective velocity of 1.33 indicates that one of three subintervals was sustained as complex, the small occupancy of this subpopulation reflects the rather small probability of association during each subinterval.

The history line formulation implicitly assumes that the probability of two transactions within one subinterval is small and, therefore, it is not necessary, in practice, to calculate the velocity distributions for pA in excess of an appropriate maximum. Kinetic rates that generate a significant probability of multiple association-dissociation reactions within a cycle subinterval are better described by a rapid equilibration formulation.

The earlier assumption of instantaneous equilibrium implied that the mixture of free and complexed components in an elemental cell could be depicted as a homogeneous population of molecules that migrate at a rate determined by a weighted average velocity of the two constituents. The kinetic algorithm represents each constituent A and B population as consisting of K subpopulations with discrete velocities ranging between the velocity of the complex and the velocity of the free constituent. At each cycle of the algorithm, the equilibrium concentrations of each cell are calculated and corrected for partial equilibrium by application of Eqs. 5 and 6. Each subpopulation is separately translated by the Gaussian protocol previously described. The concentration of each subpopulation is obtained by linear interpolation between the $c(\sigma_v)$ values that bracket the pA calculated on the basis of k_f and by the total constituent concentrations of the elemental cell. The diffusion process remains as previously described.

RESULTS AND DISCUSSION

Test of stochastic kinetic formulation

Eqs. 13–15 provide estimates of the association and dissociation probabilities used to calculate intermixing of free and complexed pools during each time-interval of the chromatography simulation. The appropriateness of these expressions was tested by comparing the time course of relaxation after dilution predicted by iterative application of the Poisson probabilities to that explicitly calculated by Eq. 5. Fig. 1 depicts the kinetics of dissociation of an equilibrated mixture diluted fourfold at time $t = 0$. Change of concentrations during each time interval were obtained from

$$\Delta a = -pA(1 - pD)a + pD(1 - pA)c \quad (22)$$

$$\Delta c = -\Delta a, \quad (23)$$

in which the decrease in concentration of a free component is determined by the product probability of *associa-*

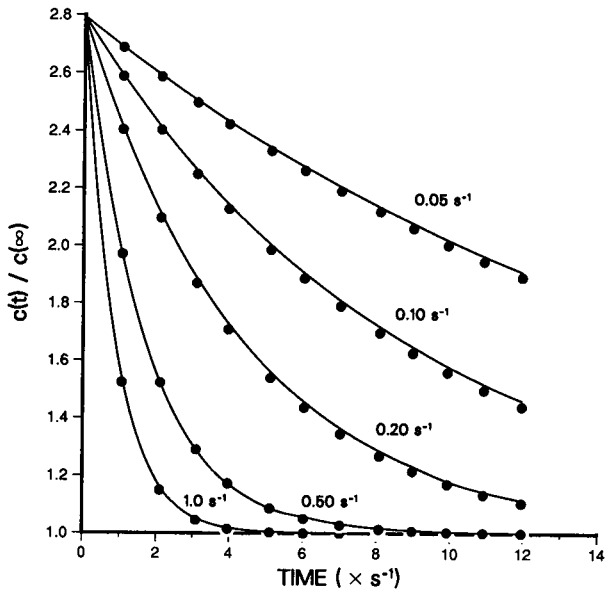

FIGURE 1 Comparison of stochastic dissociation formulation (●) with calculated dissociation (—).

tion and *not-dissociation* and, similarly, the increase in concentration is given by the product probability of *dissociation* and *not-association*. The agreement between the explicitly calculated kinetics of relaxation and the kinetics obtained by the iterative procedure shown in Fig. 1 for several values of rate constants, was taken to support the use of the Poisson expressions to approximate the extent of complex and free-molecule pool mixing during iteration time intervals in the chromatography algorithm.

Characterization of the velocity distribution function

Velocity distributions as a function of k_r for fixed probabilities of association are shown in Fig. 2. The velocity of the aggregate is arbitrarily set at 2 cells/cycle (c/c), and that for the free component at 1 c/c. Distribution functions are shown for low (pA = 0.1), intermediate (0.5), and high (0.9) probabilities of association. Note, for instance, that pA set at 0.5 indicates that k_f and constituent concentrations are such that during the subinterval, free components have equal probabilities of associating or not associating. This situation is independent of the probability of dissociation.

The shape of the velocity distribution function is in each case dependent upon the value of k_r. The most slowly dissociating sample is characterized by an asymmetric velocity distribution with the bulk of the complex migrating with the assigned velocity of the aggregate. Both velocity distribution functions generated for the more rapidly dissociating systems exhibit a quasisymmetric nature. The distribution obtained for the high value of association probability should be taken as illustrative only; for pA = 0.9, the probability of two association events during a subinterval may also be high (0.81 pD) and contradicts a fundamental assumption of the formulation. In practice, pA should be restricted to values of 0.2 or less, which may be accomplished by appropriate selection of iteration cycles per run.

The resolution of the velocity distribution function determined by the binary history line algorithm is given by the number of subpopulation discrete velocities into which the content of an elemental cell may be fragmented. To subdivide the population into subsets according to proportional velocity differences of $(1/K)$ requires K elements in the binary history line. K elements generate 2^K possible history line or event line outcomes. As a result, increased resolution in the calculation is obtained at the cost of exponentially increasing expenditure in computing time required to generate the velocity distribution matrix. Whereas a resolution of 0.1 proportional velocity units is obtained by evaluating a set of 1,024 different history lines, a twofold increase in resolution to 0.05 proportional

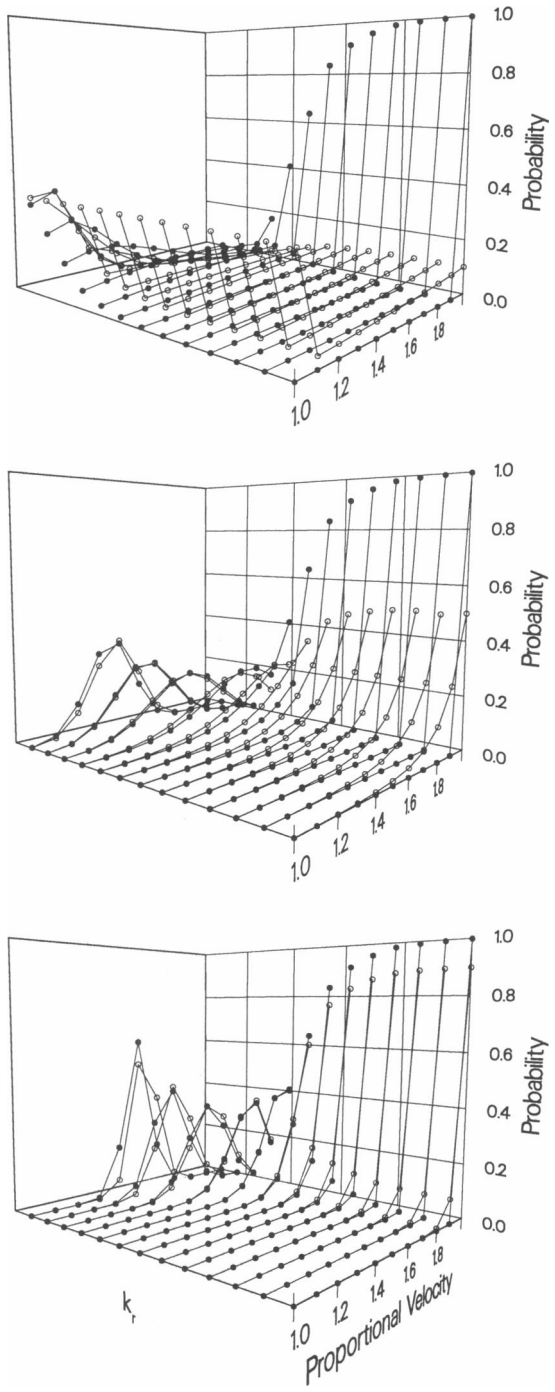

FIGURE 2 Proportional velocity distributions for complex (●) and free constituent (○) for k_r values 0.0002, 0.0005, 0.001, 0.002 . . . , 2.0 s^{-1} (front to back). Run time and free component concentrations are assumed to be such as to result in a probability of association of 0.1 (*top*), 0.5 (*middle*), and 0.9 (*bottom*) during each iteration subinterval. Each iteration cycle is subdivided into 10 subintervals.

units requires more than 10^6 history lines. In addition, the computing time expended for the iterative simulation of the chromatography run increases approximately proportionally to the number of subintervals. Therefore, it is important that a pragmatic choice for effective resolution be made.

Fig. 3 illustrates the effect of the choice of subinterval number on the resulting simulated elution profile for relatively rapidly associating-dissociating proteins. With no subdivision of the cycle interval (i.e., one subinterval) two subpopulations representing effectively stable complexed and free constituents are produced. The profiles generated, therefore, exhibit an anomalous elution behavior that would be predicted if no intermixing of free and complexed pools during an iteration cycle was incorporated into the algorithm. Absence of intermixing results in a retardation in the predicted elution rate of the solute that originates in the imposition of the intrinsic free molecule constituent velocity on a portion of the solute population during each cycle of the iteration. In contrast, rapid intermixing of pools, as indicated in Fig. 2, generates effective constituent velocities for both complex and free solutes that are intermediate between the assigned constituent velocities. The rate of solute dilution is thereby decreased, enhancing the ratio of complex in the sample, and no portion of the mixture migrates as slowly as the free solute in the absence of simulated intermixing.

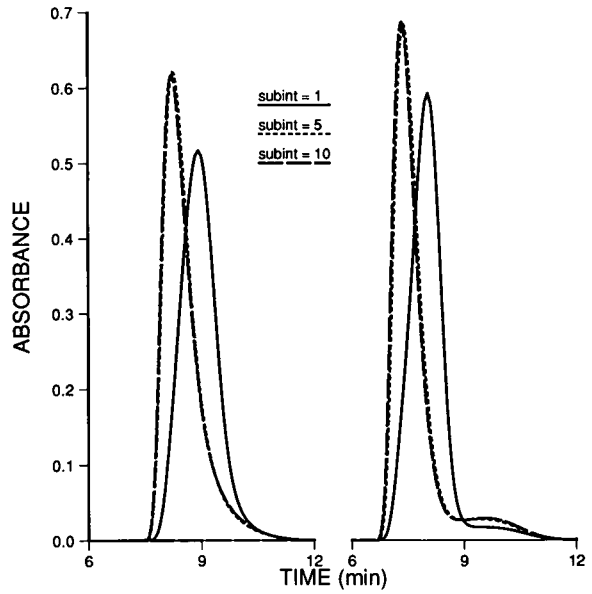

FIGURE 3 Dependence of simulated elution profiles on choice of number of subintervals per iteration cycle. Column length set to 90 cells; run length is 100 cycles; run time is 15 min; $k_r = 0.2\ s^{-1}$; $K_a = 10^5\ M^{-1}$; $a = b = 2 \times 10^{-5}$ M; sample size is two cells. (*Left*) Constituent velocities $v_a = v_b = 1.5$ cells/cycle (c/c), $v_c = 2.1$ c/c; (*right*) $v_a = 1.5$, $v_b = 2.0$, and $v_c = 2.5$ c/c. Simulated elution profiles resulting for 1 (- - - -), 5 (———), or 10 (— —) subintervals/iteration cycle are shown. Absorbances are based on an arbitrary extinction of 1.0/1.0 mg ml^{-1}.

In the two cases illustrated, homogeneous association of interacting solutes of equal velocities and mixed association by solutes of unequal constituent velocities, little change in simulated elution characteristics is exhibited when the number of subintervals per cycle is increased from 5 to 10. The chromatography behavior of solutes of unequal constituent velocities is more sensitive to the number of subintervals as a consequence of the ability of the chromatography matrix to separate dissociated molecules and thereby attenuate intermixing. In either case, the contribution of intermixing of pools diminishes as the kinetic rates decrease, reducing the probabilities of multiple dissociations during one simulation iteration cycle. As noted, the computing resources required by the algorithm are quite sensitive to the choice of subinterval value. For instance, the three runs in each case shown here required ~23, 66, and 124 s of Cray-2 CPU time for subinterval assignments of 1, 5, and 10, respectively. It is likely that future versions of the algorithm will select optimal subinterval values on the basis of k_r and run time. However, for the purpose of consistency among the illustrations presented in this study and to conserve computer processing time, history lines of five elements were chosen to represent the intermixing of pools of free and complexed molecules.

Prediction of large-zone leading boundary profiles

No explicit mathematical formulation of the small-zone elution behavior of interacting solutes has been presented and may not be possible (8, 14, 20–22). Detailed studies have been undertaken to describe the chromatography characteristics of interacting molecules during ultracentrifugation and large-zone gel filtration (1, 5–9, 23–31). In the large-zone chromatography method, a plateau of constant protein concentration allows for the construction of solute continuity equations that may be solved numerically and yield simulated elution patterns that correspond well with experimental observation (32, 33).

Therefore, the ability of the small-zone simulation to predict kinetically dependent large-zone leading boundary behavior previously calculated by Zimmerman (11) was used as a criterion by which to evaluate the soundness of the approach. A large-zone solute condition was accomplished by setting the simulated sample size at 50 cells with the column size set at 90 cells. As shown in Fig. 4, small values of k_r result in a biphasic elution profile; increasing values of k_r diminish the resolution of two distinct leading edges until only a single leading boundary is observed. In agreement with Zimmerman (11), this

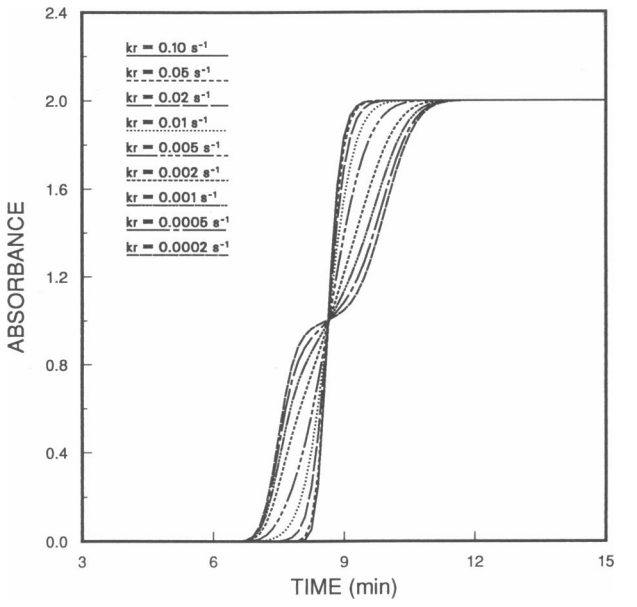

FIGURE 4 Large-zone leading boundary profiles as a function of dissociation rate constant for fixed equilibrium constant. Sample size was set at 50 cells. Simulation assumes initial concentrations of 1.0 mg/ml for two proteins of mol wt 50,000. Initial sample composition was 50% free and 50% complexed components $K_a = 10^5\ M^{-1}$. Constituent velocities are taken as 1.5 cells/cycle for free constituents and 2.1 for complex; other parameters as in Fig. 3. Fixed equilibrium constant requires that forward rate constant varies proportionally to the reverse rate constant. With increasing rate constant, the leading edge boundary shifts from a bimodal to a unimodal profile.

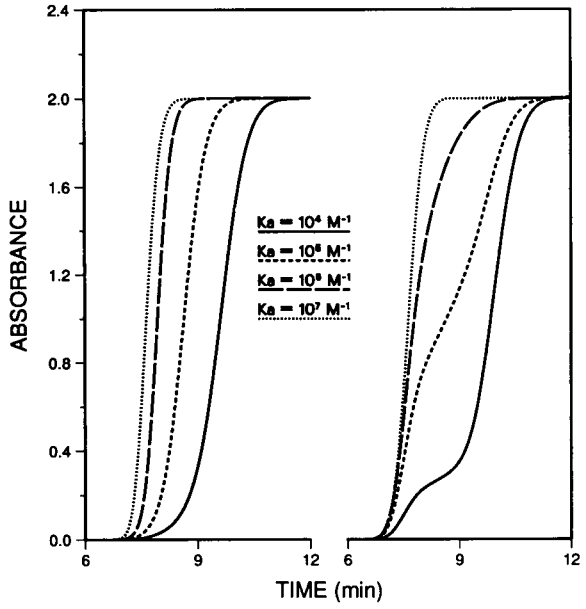

FIGURE 5 Comparison of leading boundary profile characteristics as a function of K_a for rapid and slow kinetics. (*Left*) $k_r = 0.01\ s^{-1}$; (*right*) $k_r = 0.001\ s^{-1}$. K_a ranges in order of magnitude increments from 10^4 to 10^7 to M^{-1}. Column and run parameters as in Fig. 3.

shift in character occurs within a range of dissociation rates comprising approximately two orders of magnitude. The plateau concentration observed for the leading edge of the most slowly equilibrating species is at 50% the total concentration and corresponds to the relative complex fraction at the values of K_a and concentrations used. The intersection of the leading boundaries at the 50% concentration point is also consistent with the behavior exhibited by the explicitly calculated profiles (11).

Fig. 5 represents the dependence of leading edge profiles on the equilibrium constant of interaction for two values of k_r separated by one order of magnitude. For the more rapidly interacting species, increasing values of K_a lead to shifts of a unimodal leading edge to positions of earlier elution time. The more slowly reacting solutes, on the other hand, exhibit a bimodal characteristic with, as would be expected, an increasing concentration in the leading profile as K_a is increased.

Characterization of the chromatography simulation

Figs. 6–10 illustrate contributions of kinetic control to simulated small-zone chromatograms. In Figs. 6 and 7,

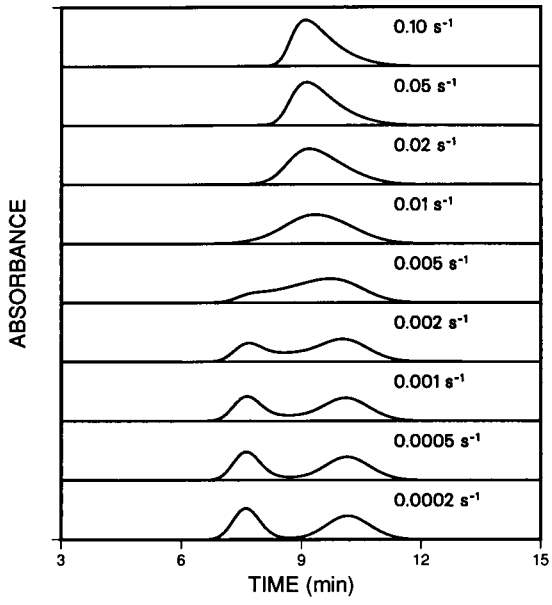

FIGURE 6 Small-zone elution profiles as a function of dissociation rate constant for fixed equilibrium constant. With increasing rate constants the nature of the chromatogram shifts from two discrete peaks at positions corresponding to 'stable' complex and free constituent to a single peak of intermediate position and exhibiting an asymmetric profile. This shift in chromatographic characteristic is effectively completed within one order of magnitude of rate constant in the range 0.001 to $0.01\ s^{-1}$.

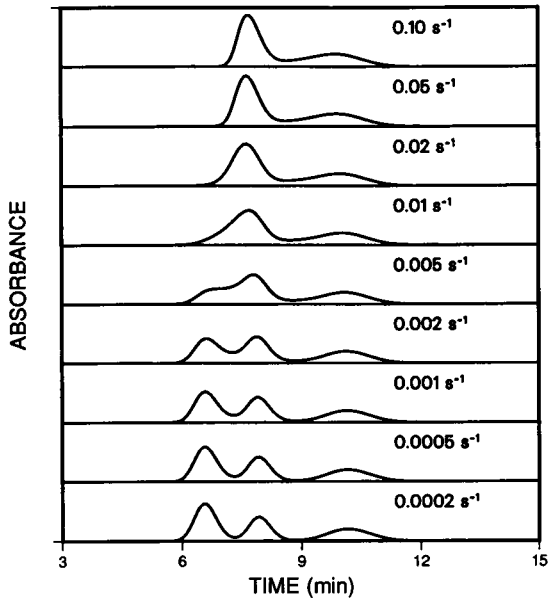

FIGURE 7 Small-zone elution profiles as a function of dissociation rate constant for fixed equilibrium constant. Simulation assumes initial concentrations of 1.0 mg/ml for two proteins of different constituent velocities. Constituent velocities are taken as 1.5 and 2.0 c/c for the two free constituents and 2.5 for complex; equilibrium constant, column length, sample size, run time, and number of iteration cycles as in Fig. 3. In descending order, rate constants are 0.1, 0.05, 0.02, 0.01, 0.005, and 0.0005 s^{-1}. The shift in elution behavior from a trimodal to a bimodal profile is effectively complete within one order of magnitude of rate constant in the range 0.001 to 0.01 s^{-1}.

the equilibrium constant is fixed and k_r is varied from 0.0002 to 0.1 s^{-1} for cases in which the associating molecules exhibit the same and different constituent elution velocities. The sample injected into the column is assumed to be at equilibrium at the initiation of the run; because K_a is fixed, the initial composition of free and complexed molecules is the same in all cases.

For interactions between molecules of the same constituent velocity (Fig. 6), the smallest reverse rate constant provides for little dissociation during the development of the chromatogram, resulting in resolution of two distinct elution peaks. Because K_a is fixed, k_f is proportionally small and little association of molecules that are initially free occurs. Hence, the second peak appears at the position expected for noninteracting molecules. As k_r is increased, the magnitude of the leading peak decreases and a continuum of material eluting between the two peaks is noted; the position of the first peak shifts to a later elution position whereas the second peak shifts to positions of earlier elution. Finally, a single peak is obtained that elutes at an intermediate position. At the highest value of k_r depicted, the observed profile is characterized by a sharp leading edge and an extended trailing edge. This elution behavior is that expected for rapidly equilibrating solutes and is consistent with behavior observed experimentally (14, 21, 34). The distinctive profile results from the rapid dissociation without reassociation experienced by complexes that migrate in advance of the bulk of the solute zone, and from diminishing rates of reassociation with decreasing concentration of reactants in the trailing edge of the solute zone.

In the examples illustrated in Figs. 6 and 7, the transition from instantaneous equilibration to kinetic control may be discerned for $k_r = 0.02\ s^{-1}$; kinetic control of the elution profile is clearly in evidence for $k_r = 0.01\ s^{-1}$. The latter corresponds to a dissociation half-life of 70 s, ~13% of the elution time (≈9 min) of the solute peak. On the basis of the simulation then, one may informally estimate that for dissociation half-lives of <5–10% the time required for elution, an assumption of 'instantaneous equilibration' is reasonable. Likewise, for half-lives on the order of the required elution time, the transition from null equilibration during chromatography to kinetically controlled chromatography becomes apparent.

Fig. 7 examines characteristics of elution behavior for interacting molecules of different constituent velocities. In the case of slow dissociation, three peaks are noted, representing the "stable" complex and the two free species. As the dissociation rate is increased, the peak representing complex is lost and, finally, two apparently independent species are observed. The presence of interaction, however, is revealed by the small but significant forward shift of each peak relative to the positions of free species observed in the chromatograms obtained with the smallest values of k_r. Because the column separates the two molecular species during periods of dissociation, opportunity to interact is lost early in the chromatography run for these molecules of relatively low affinity; therefore, the single asymmetric profile obtained in Fig. 6 is not found in this case.

In both Figs. 6 and 7, it is noted that the transition from either two distinct elution peaks to one, or from three to two, occurs in a relatively small range of k_r. Therefore, it is apparent that depending upon the absolute values of k_r and k_f, interacting molecules of the same affinity could exhibit very different elution characteristics. Similarly, molecules of different affinity might display superficially similar elution behavior.

Fig. 8 compares simulated chromatograms for interactions between molecules with fixed values of k_r but different affinities and, hence, different values of k_f. Consistent with the behavior observed in Fig. 5 depicting the K_a dependence of the large zone elution behavior, relatively small changes in the value of k_r lead to significant qualitative change in the nature of the observed elution patterns. The more rapidly equilibrating mixture

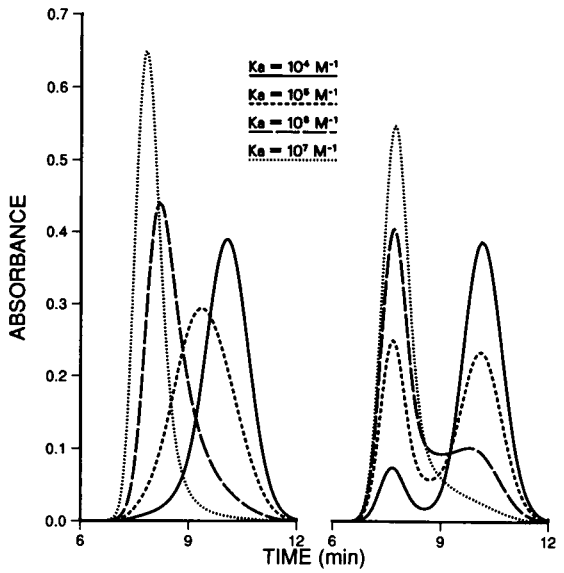

FIGURE 8 Small-zone profiles as a function of affinity constant. Chromatographic behavior is depicted in two cases distinguished by one order of magnitude difference in rate constants. In the case of the slower kinetics (*right*, $k_r = 0.001\ s^{-1}$) two distinct components in the chromatogram are observed; changes in the affinity constant result in different distributions of material at the positions of stable complex and free constituents. In the case of the faster kinetics (*left*, $k_r = 0.01\ s^{-1}$), a single elution peak is demonstrated; changes in affinity constant result in different elution positions. Sample concentrations and simulated column characteristics are as in Fig. 3.

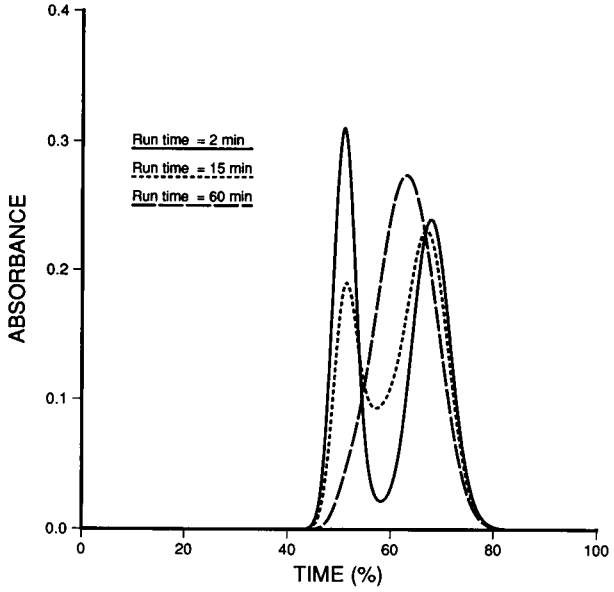

FIGURE 9 Small-zone profiles as a function of chromatogram run time. Parameters are as in Fig. 3. Chromatograms generated for simulated run times of 2, 15, and 60 min are illustrated for $k_r = 0.01\ s^{-1}$. Elution profiles are highly dependent upon flow rate (run time), shifting from two peaks to a single peak in this range.

migrates as a single asymmetric peak for which the shape and position are dependent upon the value of K_a. With a value of k_r one order of magnitude smaller, the elution profile consists of two distinct peaks, the positions of which do not change with K_a although the relative concentration of the complex peak increases with K_a.

In Fig. 9, values for reaction rate constants are fixed while the run time for the simulated chromatograms is increased. With increased run time, the relative "instantaneousness of equilibration" is also increased. This increase results in a transition in the character of the simulated elution profile from that observed previously for a small value of k_r to that obtained with a large value of k_r. For the purposes of this illustration, the values of dispersion and diffusion factors were held constant in the series of simulated profiles. Although the qualitative run-time dependence as illustrated is not jeopardized, dispersion and diffusion contributions will differ in runs in which the flow rate/run time are changed. Chromatographic dispersion decreases with flow rate, limiting the band-spreading and dilution of the solute from this source. However, the resulting increased run time increases the contribution of diffusion to band spreading. There is no reason to expect the two trends to compensate for each other.

Concentration dependence of elution profiles as experimental variable for kinetic analysis

The obvious experimental parameter to vary in a chromatographic study of interaction kinetics is the column run time as determined by the solvent flow rate. However, as discussed by Zimmerman (11) and noted above, change of flow rate is actually a change of several variables due to the dependence of chromatographic dispersion on flow characteristics and the dependence of diffusion upon time. As noted in Eq. 6, the relaxation half-life is concentration dependent. Therefore, it may be expected that both affinity and kinetic characteristics of interacting systems might be revealed in studies of the concentration dependence of elution behavior.

At equilibrium, two equimolar sets of interacting proteins of the same affinity have the same composition of complex and free molecules. Therefore, differences in elution behavior observed for proteins of the same affinity as a function of concentration result from differences in kinetic rate constants. Simulated chromatograms presented in Fig. 10 illustrate this. Consider an antigen interacting with the same affinity with two different antibodies. Although the interactions are characterized

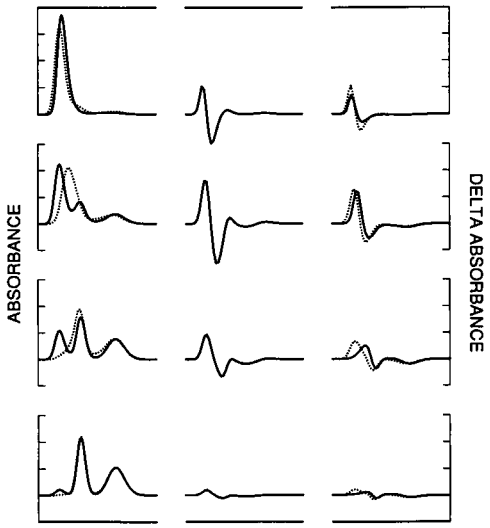

FIGURE 10 Concentration dependence of kinetically expressed elution characteristics, from top to bottom each reactant is present at a concentration of 1.0, 0.1, 0.01, 0.001 mg/ml. (*Left*) Comparison of elution profiles of two interacting systems of identical K_a (4×10^6 M^{-1}) but differing by one order of magnitude in k_r (*solid line*, $k_r = 0.01$ s^{-1}; *dotted line*, $k_r = 0.001$ s^{-1}). (*Center*) Delta profiles generated by the differences in the two elution profiles as a function of concentration. The delta profiles show a positive leading peak because the chromatogram of the more rapid kinetic system was subtracted from that of the slower. (*Right*) Comparison of delta profiles of protein 1 ($K_a = 4 \times 10^6$ M^{-1}) relative to two other interactions of higher affinity ($K_a = 10^7$ M^{-1}). In one case the increased affinity is effected by increased k_f (*solid line*), the other by decreased k_r (*dotted line*).

by the same affinity ($K_a = 4 \times 10^6$ M^{-1}), the interaction with antibody 1 is characterized by $k_r = 0.01$ s^{-1}, whereas the interaction with antibody 2 exhibits slower kinetics mediated by $k_r = 0.001$ s^{-1}. At the highest initial concentration shown, the two elution profiles exhibit similar single peaks at a position representative of the complex. However, as more dilute mixtures are chromatographed, the two elution profiles are distinguishable. The mixture characterized by the more rapid kinetics migrates as a single leading peak, whereas the mixture with smaller k_r is dispersed into two peaks.

The center column of Fig. 10 depicts delta profiles (14, 35) generated by subtraction of the elution profiles resulting from the interaction of antigen with antibody 1 from those shown for the series obtained with antibody 2. The positive leading peak observed in each case reveals the presence of higher concentrations of complex in the antibody 2 sample. Because the mixtures were assumed to be equilibrated and equivalent at the initiation of the run, the retention of complex during the run results from the slower kinetic characteristics of antibody 2. In the right panel of Fig. 10, antibody 1 is used to generate delta profiles with two antibodies of higher affinity, $K_a = 10^7$ M^{-1}. In one case, the increase in affinity is obtained through increased association rate ($k_f = 10^5$ $M^{-1}s^{-1}$). In the other case, the increase in affinity is effected by decreased dissociation ($k_r = 0.004$ s^{-1}). Again, the interacting system characterized by the slower kinetics is clearly indicated by the enhanced retention of high–molecular weight components at the lower concentrations. These differential and quantifiable chromatography chracteristics suggest that systematic concentration studies may resolve k_r and k_f contributions and provide appropriate data for experimental studies in which simulated chromatograms may be used to quantitatively evaluate the kinetic rate constants.

Validity and utility of simulation

Two aspects are relevant for discussion of the suitability of the simulation. The computer algorithm appears fundamentally sound in terms of generating chromatograms that qualitatively agree with the results of earlier studies of large-zone chromatography characteristics and, for small-zone solutes, reproduce the asymmetric single peak expected for rapidly equilibrating molecules. However, other aspects of the algorithm will be addressed as this approach is adapted to quantitative analysis of experimental data by optimized fitting of simulated chromatograms. For instance, refinement of the protocol for selection of appropriate number of iteration-cycle subintervals and other optimization of algorithm design to improve computing speed will increase usefulness of the simulation. The current diffusion algorithm will be replaced by incorporation of physical diffusion coefficients for constituents and complexes. In addition, the problem of numerical dispersion (6, 14) will be examined more closely.

Although the computational algorithm can probably be made to conform as closely to the physical processes being modeled as availability of computing resources justify, a more basic question can be raised. Weiss (36) suggested that affinity chromatography involving immobilized ligand was not an appropriate method to evaluate kinetic rate constants as suggested by Denizot and Delaage (37) in developing a stochastic formulation of affinity chromatography analogous to the chromatography theory derived earlier by Giddings and Eyring (38). The difficulties envisioned by Weiss largely originate in multiplicity of binding site classes and steric effects caused by the proximity of the matrix to the ligand. Although the gel-filtration methods do not use an immobilized component of the interaction, and therefore should be less vulnerable to these artifactual perturbations of apparent physicochemical quantities, it is nevertheless probably reasonable that no gel filtration method can measure

either the true affinity constant or true kinetic constants. That is, if it is assumed that the properties of chemically homogeneous preparations of biological macromolecles expressed in dilute solution accurately characterize molecules that evolved to function optimally as heterogeneous mixtures in a chemical environment of high excluded volume (39) and physical obstruction, then it is correct that rate constants characterizing interaction behavior in a size-exclusion medium may not be equivalent to the thermodynamically ideal rate constants.

For example, if it is correct that gel-filtration accomplishes partitioning of macromolecules on the basis of differential steric exclusion of different size molecules from portions of the mobile phase, then it may be inferred that if a molecule A is transiently located in a portion of mobile phase from which complex C is excluded, then molecule B is likewise excluded from concurrent occupancy with A. Therefore, unless B encounters A in such manner that both molecules are fortuitously aligned for productive collision, then the presence of the gel filtration matrix may have, in some sense, altered the outcome of the collision. A formulation representing the effect of the matrix on apparent rate constants and equilibrium constants has been presented by Giddings (40).

The considerations noted above apply to all forms of gel filtration–based analyses of macromolecular interaction whether kinetically controlled or rapidly equilibrating, and including both small-zone and large-zone techniques and various zonal saturation/depletion application (41–44). Nevertheless, if the potential complications involved in comparing the absolute values of rate and affinity constants determined chromatographically with those obtained by other methods are kept in mind, the usefulness of chromatography is not diminished. Techniques based on HPLC with its short analysis times, high sensitivity, small consumption of sample, and suitability for computerized and automated operation will contribute to efficient, systematic study of families of related proteins.

HPLC-based methods may be of particular usefulness for rapid qualitative and quantitative analyses of monoclonal antibodies (or their antigen binding fragments) specific for multiple epitopes on a single antigen. Variations in the affinities of antibodies for macromolecules are typically associated with the value of k_r (45, 46) with a restricted range of typical values of k_f (10^4–10^6 $M^{-1}s^{-1}$). These data should contribute to efficient application of monoclonal antibodies in immunoassay and immunotherapy processes. Moreover, knowledge of the physical chemical characteristics of antibody binding characteristics is necessary for a mechanistic understanding of the biological expression of antibodies both in recognizing antigen and in interacting with lymphocyte surface receptor.

CONCLUSIONS

The simulation described in this report, although framed in terms of size-exclusion HPLC analyses of protein interactions for convenience in experimental applications in this laboratory, imposes no explicit limitations on the transport technique used. Migration of solute is depicted in terms of constituent velocities of interacting components and complex. As in the previous study (14), no mechanism of partitioning is incorporated in the model. In principle, then, other transport processes including ultracentrifugation, electrophoresis, and field flow fractionation may provide data suited for analysis by this simulation approach. The essential requirement is that at least one of the three components of the mixture, i.e., the complex and two free constituents, exhibits a partitioning coefficient different than the others thereby assuring that interactions between the two constituents generate an elution profile of a mixture that is different than the summed profiles of the constituents chromatographed individually.

Results of the simulation indicate that under appropriately selected conditions of run time, observed elution profiles are sensitively related to the kinetic rates of association and dissociation. For an appropriately selected run time, variation of the solute concentration systematically generates elution profiles whose shapes are determined by the kinetics of the interaction. Comparative inspection of elution profiles exhibited by multiple interacting pairs of proteins yields qualitative rankings of relative contributions of reverse and forward rate constants. Quantitative interpretation of elution profiles observed experimentally will be addressed after further refinement of the simulation.

I thank Dr. D. Haugen and Dr. M. Schiffer for critical reading of this manuscript and Mrs. Carol Fox for assistance with computer graphics.

This work was supported by the United States Department of Energy, Office of Health and Environmental Research, under Contract W-31-109-ENG-38.

Received for publication 2 December 1988 and in final form 23 February 1989.

REFERENCES

1. Bethune, J. L., and G. Kegeles. 1961. Countercurrent distribution of chemically reacting systems. I. Polymerization. *J. Phys. Chem.* 65:433–438.
2. Dishon, M., G. H. Weiss, and D. A. Yphantis. 1966. Numerical

solutions of the Lamm equation. II. Equilibrium sedimentation. *Biopolymers.* 4:457–468.

3. Cann, J. R. 1970. Interacting Macromolecules. The Theory and Practice of their Electrophoresis, Ultracentrifugation, and Chromatography. Academic Press, New York.
4. Cann, J. R., and W. B. Goad. 1972. Theory of sedimentation for ligand-mediated dimerization. *Arch. Biochem. Biophys.* 153:603–609.
5. Cox, D. J. 1971. Computer simulation of sedimentation in the ultracentrifuge. V. Ideal and non-ideal monomer-trimer systems. *Arch. Biochem. Biophys.* 142:514–526.
6. Cox, D. J. 1978. Calculation of simulated sedimentation velocity profiles for self-associating solutes. *Methods Enzymol.* 48:212–242.
7. Zimmerman, J. K., and G. Ackers. 1971. Molecular sieve studies of interacting protein systems. VI. Effects of axial dispersion on boundary profiles of associating macromolecules. *J. Biol. Chem.* 246:1078–1087.
8. Zimmerman, J. K., and G. Ackers. 1971. Molecular sieve studies of interacting protein systems. X. Behavior of small zone profiles for reversibly self-associating solutes. *J. Biol. Chem.* 246:7289–7292.
9. Cann, J. R. and D. C. Oates. 1973. Theory of electrophoresis and sedimentation for some kinetically controlled interactions. *Biochemistry.* 12:1112–1119.
10. Cann, J. R., and G. Kegeles. 1974. Theory of sedimentation for kinetically controlled dimerization reactions. *Biochemistry.* 13:1868–1874.
11. Zimmerman, J. K. 1974. Kinetically controlled association-dissociation reactions on gel chromatography. *Biochemistry.* 13:384–389.
12. Endo, S., H. Hayashi, and A. Wada. 1982. Affinity chromatography without immobilized ligands: a new method for studying macromolecular interactions using high-performance liquid chromatography. *Anal. Biochem.* 124:372–379.
13. Endo, S., and A. Wada. 1983. Theoretical and experimental studies on zone-interference chromatography as a new method for determining macromolecular kinetic constants. *Biophys. Chem.* 18:291–301.
14. Stevens, F. J. 1986. Analysis of protein-protein interaction by simulation of small-zone size-exclusion chromatography: application to an antibody-antigen association. *Biochemistry.* 25:981–993.
15. Stevens, F. J., W. E. Carperos, W. J. Monafo, and N. S. Greenspan. 1988. Size-exclusion HPLC analysis of epitopes. *J. Immunol. Methods.* 108:271–278.
16. Baudin-Chich, V., M. Marden, and H. Wajcman. 1988. Investigation of the tetramer-dimer equilibrium in haemoglobin solutions by high-performance size-exclusion chromatography on a diol column. *J. Chromatogr.* 437:193–201.
17. Nimmo, I. A., and A. Bauermeister. 1978. A theoretical analysis of the use of zonal gel filtration in the detection and purification of protein-ligand complexes. *Biochem. J.* 169:437–440.
18. Cann, J. R., E. J. York, J. M. Stewart, J. C. Vera, and R. B. Maccioni. 1988. Small zone gel chromatography of interacting systems: theoretical and experimental evaluation of elution profiles for kinetically controlled macromolecular-ligand reactions. *Anal. Biochem.* 175:462–473.
19. Giddings, J. C. 1957. Stochastic considerations on chromatographic dispersion. *J. Chem. Phys.* 26:169–173.
20. Ackers, G. K. 1975. Molecular sieve methods of analysis. *In* The Proteins. Vol. 1. H. Neurath and R. L. Hill, editors. Academic Press, Inc., New York. 1–94.
21. Stevens, F. J., F. A. Westholm, A. Solomon, and M. Schiffer. 1980. Self-association of human immunoglobulin κI light chains: role of the third hypervariable region. *Proc. Natl. Acad. Sci. USA.* 77:1144–1148.
22. Stevens, F. J., and M. Schiffer. 1981. Computer simulation of protein self-association during small-zone gel filtration. Estimation of equilibrium constants. *Biochem. J.* 195:213–219.
23. Gilbert, G. A., and R. C. Jenkins. 1959. Sedimentation and electrophoresis of interacting substances. II. Asymptotic boundary shape for two substances interacting reversibly. *Proc. R. Soc. Lond. A.* 253:420–437.
24. Nichol, L. W., and A. G. Ogston. 1965. A generalized approach to the description of interaction boundaries in migrating systems. *Proc. R. Soc. Lond. B.* 163:343–368.
25. Ackers, G. K. 1964. Molecular exclusion and restricted diffusion processes in molecular sieve chromatography. *Biochemistry.* 3:723–730.
26. Ackers, G. K., and T. E. Thompson. 1965. Determination of stoichiometry and equilibrium constants for reversibly associating systems by molecular sieve chromatography. *Proc. Natl. Acad. Sci. USA.* 53:342–349.
27. Cox, D. J. 1967. Computer simulation of sedimentation in the ultracentrifuge. III. Concentration-dependent sedimentation. *Arch. Biochem. Biophys.* 119:230–239.
28. Cox, D. J. 1969. Computer simulation of sedimentation in the ultracentrifuge. IV. Velocity sedimentation of self-associating solutes. *Arch. Biochem. Biophys.* 129:106–123.
29. Zimmerman, J. K., D. J. Cox, and G. Ackers. 1971. Molecular sieve studies of interacting protein systems. IX. Reaction boundary profiles for monomer-*n*-mer systems: comparison with sedimentation. *J. Biol. Chem.* 246:4242–4250.
30. Kegeles, G., and J. R. Cann. 1978. Kinetically controlled mass transport of associating-dissociating macromolecules. *Methods Enzymol.* 48:248–270.
31. Chatelier, R. C., and A. P. Minton. 1981. Sedimentation equilibrium in macromolecular solutions of arbitrary concentration. I. Self-associating proteins. *Biopolymers.* 20:2093–2120.
32. Winzor, D. J. 1981. Mass migration methods. *In* Protein-Protein Interactions. C. Frieden and L. W. Nichol, editors. John Wiley and Sons, New York. 129–172.
33. Cox, D. J., and R. S. Dale. 1981. Simulation of transport experiments for interacting systems. *In* Protein-Protein Interactions. C. Frieden and L. W. Nichol, editors. John Wiley and Sons, New York. 173–212.
34. Winzor, D. J., and H. A. Scheraga. 1963. Studies of chemically reacting systems on Sephadex. I. Chromatographic demonstration of the Gilbert theory. *Biochemistry.* 2:1263–1267.
35. Stevens, F. J., D. A. LeBuis, W. J. Eisler, and C. F. Ainsworth. 1986. Macromolecular interactions: application of microcomputer-controlled, high speed size-exclusion chromatography. *LCGC.* 4:340–348.
36. Weiss, G. H. 1981. Can one measure rate constants using chromatographic methods? *Sep. Sci. and Technol.* 16:75–80.
37. Denizot, F. C., and M. A. Delagge. 1975. Statistical theory of chromatography: new outlooks for affinity chromatography. *Proc. Natl. Acad. Sci. USA.* 72:4840–4843.
38. Giddings, J. C., and H. Eyring. 1955. A molecular dynamic theory of chromatography. *J. Phys. Chem.* 59:416–421.

39. Minton, A. P. 1981. Excluded volume as a determinant of macromolecular structure and reactivity. *Biopolymers.* 20:2093–2120.

40. Giddings, J. C. 1970. Effect of membranes and other porous networks on the equilibrium and rate constants of macromolecular reactions. *J. Phys. Chem.* 74:1368–1370.

41. Hummel, J. P., and W. J. Dreyer. 1962. Measurement of protein-binding phenomena by gel filtration. *Biochim. Biophys. Acta.* 63:530–532.

42. Oshima, G., H. Uchiyama, and K. Nagasawa. 1981. A new method for determining the dissociation constant between macromolecules by gel permeation. *Anal. Biochem.* 111:366–371.

43. Frankel, A. D., G. K. Ackers, and H. O. Smith. 1985. Measurement of DNA-protein equilibria using gel chromatography: application to the *Hinf*1 restriction endonuclease. *Biochemistry.* 24:3049–3054.

44. Mahieu, J.-P., B. Sebille, C. T. Craescu, M.-D. Rhoda, and Y. Beuzard. 1985. Determination of the dissociation constant of oligomeric proteins by size-exclusion high-performance liquid chromatography: application to human hemoglobin. *J. Chromatogr.* 327:813–825.

45. Froese, A. 1968. Kinetic and equilibrium studies on 2,4-dinitrophenyl hapten-antibody systems. *Immunochemistry.* 5:253–264.

46. Pontarotti, P. A., R. Rahmanni, M. L. Martin, and J. Barbet. 1985. Monoclonal antibodies to antitumor vinca alkaloids: thermodynamics and kinetics. *Mol. Immunol.* 22:277–284.